Journal of Ultrafine Grained and Nanostructured Materials
https://jufgnsm.ut.ac.ir
Vol. 59, No.1, June 2026, pp. 161-185
Print ISSN: 2423-6845 Online ISSN: 2423-6837
DOI: 10.22059/jufgnsm.2026.01.12

Fabrication and Characterization of Aluminum Matrix Composite Tubes Reinforced with Continuous Glass Fibers via Filament Winding Method

Ali Alizadeh[1,*], Ali Zeinali[1], Mohsen Heydari Beni[1], Jafar Eskandari Jam[1], Majid Eskandari Shahraki[2], Alireza Asadolahei[3]

[1]Faculty of Materials and Manufacturing Technologies, Malek Ashtar University of Technology, Tehran, Iran.
[2]Department of Aerospace Engineering, Faculty of Engineering, Ferdowsi University of Mashhad, Mashhad, Iran.
[3]Mechanical Engineering Department, Faculty of Engineering, Imam Khomeini International University, Qazvin, Iran.

Recieved: 1 January 2026; Accepted: 25 April 2026

[*]Corresponding author, E-mail: a_alizadeh@mut.ac.ir

ABSTRACT

This study investigates the fabrication of aluminum matrix composite (AMC) tubes reinforced with continuous glass fibers using the filament winding technique. Owing to the weak wettability and poor interfacial bonding between molten aluminum and glass fibers, surface modification of the fibers was employed to enhance fiber–matrix interaction. For this purpose, an electroless nickel–phosphorus (Ni–P) coating was deposited on the glass fibers from an acidic bath. The coated fibers were subsequently heat treated at 300 °C, 370 °C, and 450 °C. The structural and thermal characteristics of the coatings, both as-deposited and heat-treated, were examined using X-ray diffraction (XRD), field emission scanning electron microscopy (FESEM), energy-dispersive spectroscopy (EDS), and differential scanning calorimetry (DSC). XRD was used to identify the formation of crystalline phases upon heat treatment, while FESEM revealed the coating morphology and fiber–matrix interface in the final composite. DSC analysis assessed the thermal stability of untreated and heat-treated coatings at filament winding temperatures. Filament winding was performed into molten pure aluminum using uncoated, coated (without heat treatment), and heat-treated fibers. Additionally, winding was carried out into molten A356 aluminum alloy using coated fibers with and without heat treatment. The results indicated that optimal winding performance occurs near the alloy's solidification temperature. Among the tested conditions, the Ni–P coating heat treated at 450 °C exhibited superior wettability and bonding characteristics for integration with molten aluminum.

Keywords: *Glass fibers, Pure aluminum, Aluminum 356 A, Nickel-phosphorus coating, Filament winding, Heat treatment.*

1. Introduction

One of the most critical industrial demands in modern engineering is the development of lightweight structures without compromising their mechanical performance. Unlike monolithic materials, metal matrix composites (MMCs) offer enhanced design flexibility and reduced weight while maintaining high strength and stiffness. These composites typically consist of a metallic matrix, such as aluminum, reinforced with long fibers such as alumina. MMCs are commonly fabricated by infiltrating molten metal into a mold containing a fiber preform. To improve infiltration, external pressure may be applied. However, the molds used in these casting processes are often expensive, and their costs increase significantly with size. An alternative and more cost-effective method involves producing fiber-reinforced composite tubes by winding aluminum strips pre-impregnated with fibers around a mandrel, thereby

eliminating the need for large-scale casting molds. A major challenge in the fabrication of MMCs reinforced with ceramic, glass, or carbon fibers is the poor wettability between the metallic melt and the reinforcement, which results in weak interfacial bonding and reduced mechanical performance. Various techniques have been proposed to improve this issue, such as filament winding in vacuum or inert atmospheres, the addition of alloying elements like magnesium or silicon to enhance wettability, and surface modification of the fibers through coating. This study focuses on improving the wettability and interfacial adhesion of molten aluminum with coated glass fibers for use in the filament winding process. Several coating techniques have been developed for this purpose, including physical vapor deposition (PVD), chemical vapor deposition (CVD), electroplating (for conductive fibers), and electroless plating. Among these, electroless nickel-phosphorus (EN-P) coating has gained attention due to its simplicity, cost-effectiveness, and favorable properties. In this work, particular emphasis is placed on investigating the effect of post-deposition heat treatment on the properties of the EN-P coating. Based on previous research [1–2], it has been shown that EN-P coatings without heat treatment exhibit inadequate interfacial bonding performance in aluminum melt infiltration during filament winding.

In a 2007 study, electroless Ni–W–P coatings were applied to glass fibers to investigate their adhesion characteristics, morphology, and phase composition [3]. The results demonstrated successful, pore-free coating deposition. Furthermore, thermal shock testing confirmed favorable resistance to delamination. A 2016 investigation focused on the electroless deposition of Ni–P coatings onto glass fibers and examined the optimization of bath parameters, including pH, temperature, deposition time, and stabilizer concentration. The study concluded that the optimal deposition temperature was 80 °C, the ideal pH range was between 9 and 9.5, and the recommended stabilizer concentration was 25 mg/L. In a 2008 study, electroless Ni–P coatings were deposited on glass fibers to impart electrical conductivity. It was observed that a minimum immersion time of 10 minutes was necessary to form a continuous metallic nickel layer on the fiber surface [4]. In another investigation from 2006, the tribological behavior and coating conditions of electroless Ni–P on potassium titanate whiskers were evaluated [5]. The findings indicated uniform and successful deposition across the whisker surfaces. A 2013 study aimed to enhance the wettability and dispersion of short basalt fibers within an aluminum matrix composite by coating the fibers with copper via the electroless process. The coating improved the uniform distribution of the fibers, minimized agglomeration, and enhanced fiber–matrix interaction. SEM analysis revealed that approximately 95% of the fibers were uniformly coated [6]. Additionally, the effect of electroless nickel coatings on SiC and Al_2O_3 particles was studied to assess their wettability with molten aluminum. Sessile drop tests showed that the contact angle decreased to 11.6° for SiC and 12.2° for Al_2O_3, attributed to differences in surface energy and chemical interaction at the interface [7].

In one study, electroless nickel plating was applied to hollow glass microspheres using hypophosphite as a reducing agent in an alkaline bath [8]. Prior surface activation using a palladium-based sensitizer facilitated uniform coating by increasing the adsorption capacity of the microspheres. Magnetic properties of the microspheres were enhanced by adjusting the pH and the concentration of the reducing agent. Morphology, composition, and structure of the deposited layer were examined, revealing that the coating thickness increased with deposition time. Post-deposition heat treatment was found to significantly improve the crystallinity of the nickel layer [2]. In another investigation, gas pressure infiltration was employed to fabricate a composite consisting of randomly oriented continuous carbon fibers coated with Ni in an aluminum 2014 alloy matrix. The resulting microstructure exhibited full infiltration of the alloy and a homogeneous fiber distribution at a volume fraction of 30%. No evidence of fiber agglomeration or residual porosity was observed. The fiber–matrix interface was smooth and free from discontinuities. EDXA analysis confirmed that no significant interfacial reactions occurred between the aluminum matrix and the fibers. Compared to the monolithic aluminum alloy, the composite showed considerable improvements in both elastic modulus and ultimate tensile strength, although the elongation to failure was notably reduced. Moreover, the measured tensile modulus and ultimate tensile strength were in good agreement with predictions from the rule of mixtures, indicating a strong fiber–matrix interface and negligible degradation of fiber strength during processing. SEM images of the fracture surfaces revealed that failure predominantly occurred within the relatively weak aluminum matrix, while fibers remained intact and unbroken. The matrix was composed of aluminum alloy 2014, containing 4.3% Cu, 1% Mn, 0.9% Mg, 0.5% Si, and balance Al. Initial attempts to fabricate the 2014Al–Cf composite using uncoated carbon fibers and gas pressure infiltration were unsuccessful due to the high surface tension of molten aluminum and the poor wettability of the fibers. To overcome these issues and avoid detrimental interfacial reactions,

carbon fibers coated with nickel were utilized [6].

The primary objectives of this study are:

-To deposit a uniform EN-P coating on E-glass fibers using an optimized electroless plating bath.

-To investigate the microstructural evolution, phase transformation, and thermal stability of the coating after heat treatment at 300°C, 370°C, and 450°C.

-To evaluate the adhesion strength of the coating under thermal shock conditions.

-To assess the in-melt winding performance of uncoated, as-coated, and heat-treated fibers in both pure aluminum and A356 aluminum alloy.

-To identify the optimal heat treatment condition that yields superior wettability and interfacial bonding for the fabrication of glass fiber-reinforced aluminum matrix composite tubes.

The novelty of this work lies in systematically investigating the effect of heat treatment on EN-P-coated E-glass fibers to enhance their wettability and adhesion with molten aluminum, specifically for the filament winding process. The central hypothesis of this research is that heat treatment at an optimized temperature will transform the amorphous EN-P coating into a crystalline structure, thereby improving its adhesion to the glass substrate and its stability in the molten metal, ultimately leading to a sound fiber-matrix interface.

2. Material and methods

2.1. Raw Materials

In this study, E-glass fibers were utilized as the primary reinforcement material and substrate for electroless nickel plating. Two different aluminum sources were used as the matrix: high-purity aluminum ingots (99% purity, supplied by Al-Mahdi Co.) and an Al-356A alloy, both serving as the matrix for the fabrication of fiber-reinforced aluminum composite tubes. For the plating substrates, standard glass microscope slides were also employed. The electroless nickel plating bath was prepared using nickel chloride ($NiCl_2$, 99% purity) as the metal ion source. Sodium hypophosphite ($NaPO_2H_2{\cdot}H_2O$, 98.5% purity) was used as the reducing agent. Boric acid (H_3BO_3, 99% purity) served as a buffering agent to maintain the bath pH and ensure bath stability. Ammonium bifluoride (NH_4HF_2, 98% purity) was added as a stabilizer. Prior to the plating process, a two-step surface activation treatment was performed. Stannous chloride ($SnCl_2$, 98% purity) and palladium chloride ($PdCl_2$, 98% purity) were used to prepare the sensitizing and activating solutions, respectively. Hydrochloric acid (HCl, 37% concentration, 99% purity) was used in the preparation of these solutions and for pH adjustment. Ammonia solution (NH_3, 25% concentration, 99% purity) was also used for pH regulation of the electroless bath.

2.2. Equipment for Electroless Plating

The electroless plating process was carried out using standard laboratory equipment, including beakers, volumetric flasks, a digital balance, magnetic stirrer with heater, oven, and thermometer. pH values were monitored using pH indicator papers. All chemicals were used without further purification, and all solutions were prepared with distilled water.

2.3. Fabrication Setup for Infiltration and Fiber Winding

To fabricate fiber-reinforced aluminum composite tubes, a custom setup was developed to perform direct fiber winding into molten aluminum under an inert argon atmosphere to prevent oxidation during both winding and subsequent heat treatment. The system incorporated a custom-built electric furnace, constructed with 3 mm Kanthal A1 heating elements (manufactured in Sweden) supported by shaped alumina refractory bricks, with the inner chamber coated using high-temperature refractory mortar (Type 60) to ensure thermal stability and insulation. The furnace components were housed within a steel casing (65 × 50 × 35 cm), and a rotating chromium steel mandrel (20 mm diameter) shaped with refractory castable material was used for fiber winding, providing resistance against high-temperature corrosion in molten aluminum. The mandrel was driven by a 0.75 HP electric motor through a 12 mm steel shaft and worm gear assembly, with rotational speed precisely controlled via an inverter. Molten aluminum was contained in a cast iron crucible positioned beneath the mandrel, and process temperatures were monitored using two thermocouples for the furnace and melt, respectively. Fire-resistant electrical connections, ceramic terminals, an insulated control panel, high-temperature insulation boards, and ceramic blankets were employed to regulate furnace operation, minimize thermal losses, and protect the furnace structure. Filament winding was conducted at 820, 770, and 720 °C, with optimal performance observed at 720 °C, where the aluminum approached semi-solid conditions, enabling improved fiber embedment and composite integrity.

2.4. Preparation of Samples and Electroless Plating Procedure

a. Fiber Cleaning and Removal of Volatile Compounds

To clean the surface of the glass fibers from potential contaminants and adhering impurities,

the fibers were immersed in deionized water for 10 minutes. After drying, they were placed in an oven at 100 °C for 1 hour to remove any volatile compounds that might be present on the fiber surface. The average coating thickness was approximately 110–120 nm, as measured from cross-sectional FESEM images. The most reliable measurement (L1) indicated a thickness of 114.68 nm.

b. Sensitization Process

To prepare the sensitizing solution, 10 g/L of stannous chloride ($SnCl_2$) was first dissolved in deionized water in a 100 mL beaker under ambient conditions using a magnetic stirrer. In a separate 100 mL beaker, a solution containing 40 mL/L hydrochloric acid (HCl) was prepared with deionized water. For a final solution volume of 250 mL, 2.5 g of $SnCl_2$ and 10 mL of HCl were used. The two solutions were mixed in a 250 mL volumetric flask and diluted to the final volume with deionized water. The cleaned fibers were then immersed in the sensitizing solution for 15 minutes.

c. Activation Process

The activation solution was prepared using a concentration of 0.2 g/L palladium chloride ($PdCl_2$) and 2 mL/L hydrochloric acid (HCl). To prepare 500 mL of the activation solution, 0.1 g of $PdCl_2$ and 1 mL of HCl were dissolved in deionized water under magnetic stirring to ensure homogeneity. After sensitization, the fibers were rinsed and immersed in deionized water for 5 minutes. Subsequently, they were placed in the activation solution for 15 minutes.

d. Final Electroless Plating Bath

In this stage, the electroless plating bath was prepared according to the optimized formulation shown in Table 1. It is noteworthy that, due to the comprehensive scope of this research, extensive experiments were conducted to determine the optimal composition of the final bath. Various formulations were tested, and the following bath composition was selected based on its superior performance. Therefore, to avoid redundancy with previously published works, the detailed evaluation of individual parameters affecting plating performance is not repeated here. The pH of the final bath was maintained in the range of 4–5, and the plating temperature was set at 90 °C.

Table 1- Final Electroless Plating Bath Composition

Material	Value (g/ L)
$NiCl_2$	12
NaH_2PO_2	10
H_3BO_3	15
NH_4F	3

2.5. Heat Treatment of Coated Fibers

In order to evaluate the effect of heat treatment on the properties of the coating as well as its influence during the fiber winding process in molten metal, Heat treatment was conducted at 300, 370, and 450 °C under argon atmosphere with a heating rate of 10 °C/min and a holding time of 60 minutes at the target temperature.

2.6. Thermal Shock Testing

The thermal shock test was performed on the electroless nickel–phosphorus coated glass fibers in accordance with ASTM E84 standard to evaluate the adhesion between the coating and the glass fibers. This test was conducted on four types of samples:

a. Coated glass fibers without heat treatment,
b. Coated glass fibers heat-treated at 300 °C,
c. Coated glass fibers heat-treated at 370 °C,
d. Coated glass fibers heat-treated at 450 °C.

For each test, the coated fibers were first heated to 200 °C and then rapidly quenched in water at room temperature. This cycle was repeated eight times for each sample.

2.7. Equipment Used for Sample Analysis

To investigate the microstructural characteristics and material behavior of the fabricated samples, several analytical techniques were employed, including X-ray Diffraction (XRD), Field Emission Scanning Electron Microscopy (FESEM), Energy Dispersive Spectroscopy (EDS), and Differential Scanning Calorimetry (DSC).

2.7.1. X-ray Diffraction (XRD) Analysis

To investigate the phase composition of the electroless-coated samples before and after heat treatment, X-ray diffraction analysis was performed using a PHILIPS PW1730 diffractometer. The step size was set to 0.05°, with a scan time of one second per step. The wavelength employed in the XRD test was 0.154 nm. Samples were analyzed according to the conditions summarized in Table 2.

2.7.2. Differential Scanning Calorimetry (DSC) Analysis

The thermal behavior of both the glass fibers and their electroless Ni–P coating was investigated using Differential Scanning Calorimetry (DSC). DSC-TG analyses were performed on a SETARAM instrument (France) under ambient atmosphere to replicate the actual conditions during filament winding in molten aluminum. Four sample types were analyzed: uncoated fibers, coated fibers, and coated fibers heat-treated at 370 °C and 450 °C.

DSC measurements were conducted from room temperature to 720 °C at a heating rate of 15 °C/ min. This heating rate was selected to achieve

Table 2- Sample Specifications for XRD Analysis

Sample No.	Sample Description
1	Uncoated glass fiber
2	Glass fiber coated with electroless Ni–P, without heat treatment
3	Glass fiber coated with electroless Ni–P, heat-treated at 300 °C
4	Glass fiber coated with electroless Ni–P, heat-treated at 370 °C
5	Glass fiber coated with electroless Ni–P, heat-treated at 450 °C
6	Electroless Ni–P coating, heat-treated at 300 °C
7	Electroless Ni–P coating, heat-treated at 370 °C
8	Electroless Ni–P coating, heat-treated at 450 °C

adequate thermal resolution while minimizing peak broadening. The DSC data were used to assess phase transformation behavior, crystallization temperature, and thermal stability of the Ni–P coating system.

2.7.3. Field Emission Scanning Electron Microscopy (FESEM)

Field emission scanning electron microscopy (FESEM) was employed to examine the microstructure of the coatings and fibers, measure the coating thickness and grain size, and assess the adhesion of the coating to the substrate as well as the adhesion of the coated fibers to the metallic matrix. The dynamic resistance and the bonding quality of the deposit were qualitatively evaluated using thermal shock testing in accordance with ASTM-84. In addition, the interfacial bonding strength of the deposit was qualitatively observed under the microscope. The FESEM analysis was carried out using a Mira 3XMU instrument manufactured by TESCAN, equipped with a large chamber and high vacuum speed, at Razi Metallurgical Research Center. This microscope is one of the most advanced FESEMs currently available in Iran, featuring three detectors that allow imaging at magnifications up to 700,000× and enable structural investigations at the nanometer scale.

2.7.4. Energy-Dispersive X-ray Spectroscopy (EDS) Analysis

The scanning electron microscope described above was equipped with a second-generation energy-dispersive X-ray spectroscopy (EDS) microanalysis system. This technique was employed to quantitatively determine the elemental composition of the phases present in the microstructure. However, it does not replace conventional elemental analysis methods. EDS is suitable for both standard-based and standardless analytical approaches, offering sufficient accuracy and precision in both cases. This method is intended for use with solid-state detectors (SSD) mounted on SEM or EPMA instruments.

2.8. Coating Deposition on Glass Slides

Due to the lack of observable crystallization behavior in the fiber coatings, the deposition process was repeated using glass microscope slides as substrates. Glass slides were selected because, first, the coating could be easily detached from their surfaces after deposition, and second, their chemical composition and structure are similar to the glass fibers used in this study. This approach enabled the analysis of the coating properties independently, without interference from the fiber substrate. Following the deposition process, XRD analysis was performed on the coated slides. Subsequently, the coatings from four different slide samples were separately detached for DSC analysis: the as-deposited coating (without heat treatment), and coatings heat-treated at 300 °C, 370 °C, and 450 °C.

2.9. Molten Aluminum Filament Winding Device

This device has no domestic equivalent and was developed based on a U.S. patent. In this setup, bundles of high-temperature-resistant fibers such as ceramic, carbon, or glass fibers are introduced from one end into the system and pass through a crucible containing molten aluminum or other low-melting-point metals (below 1200 °C). As the fibers traverse the molten metal, they become wetted, and due to the partial submersion of a rotating mandrel in the molten bath, both the liquid metal and the fiber bundle pre-impregnated with the molten phase are simultaneously wound onto the mandrel. The winding continues until the desired composite wall thickness is achieved. Finally, the formed composite shell is removed from the mandrel and, if necessary, subjected to post-heat treatment depending on the alloy used.

Several samples were produced using this custom-built molten aluminum filament winding device under different experimental conditions:

a. Filament winding in molten pure aluminum

using uncoated fibers at various temperatures.
b. Filament winding in molten pure aluminum using coated glass fibers without heat treatment.
c. Filament winding in molten pure aluminum using coated glass fibers heat-treated at 450 °C.
d. Filament winding in molten aluminum alloy 356A using coated fibers without heat treatment at various temperatures.
e. Filament winding in molten 356A alloy using coated fibers heat-treated at 300 °C.
f. Filament winding in molten 356A alloy using coated fibers heat-treated at 370 °C.
g. Filament winding in molten 356A alloy using coated fibers heat-treated at 450 °C.

3. Results and Discussion

3.1. X-ray Diffraction (XRD) Analysis of Coated and Uncoated Fibers

XRD analysis was performed on the uncoated glass fibers to confirm their amorphous structure. As expected, the XRD pattern presented in Figure 1-A indicates the amorphous nature of the glass fibers used in this study. Additionally, XRD was carried out on the electroless Ni–P coated fibers without heat treatment to verify the amorphous nature of the coating. One of the key characteristics of electroless Ni–P coatings is their amorphous structure, which is clearly reflected in the XRD pattern shown in Figure 1-B.

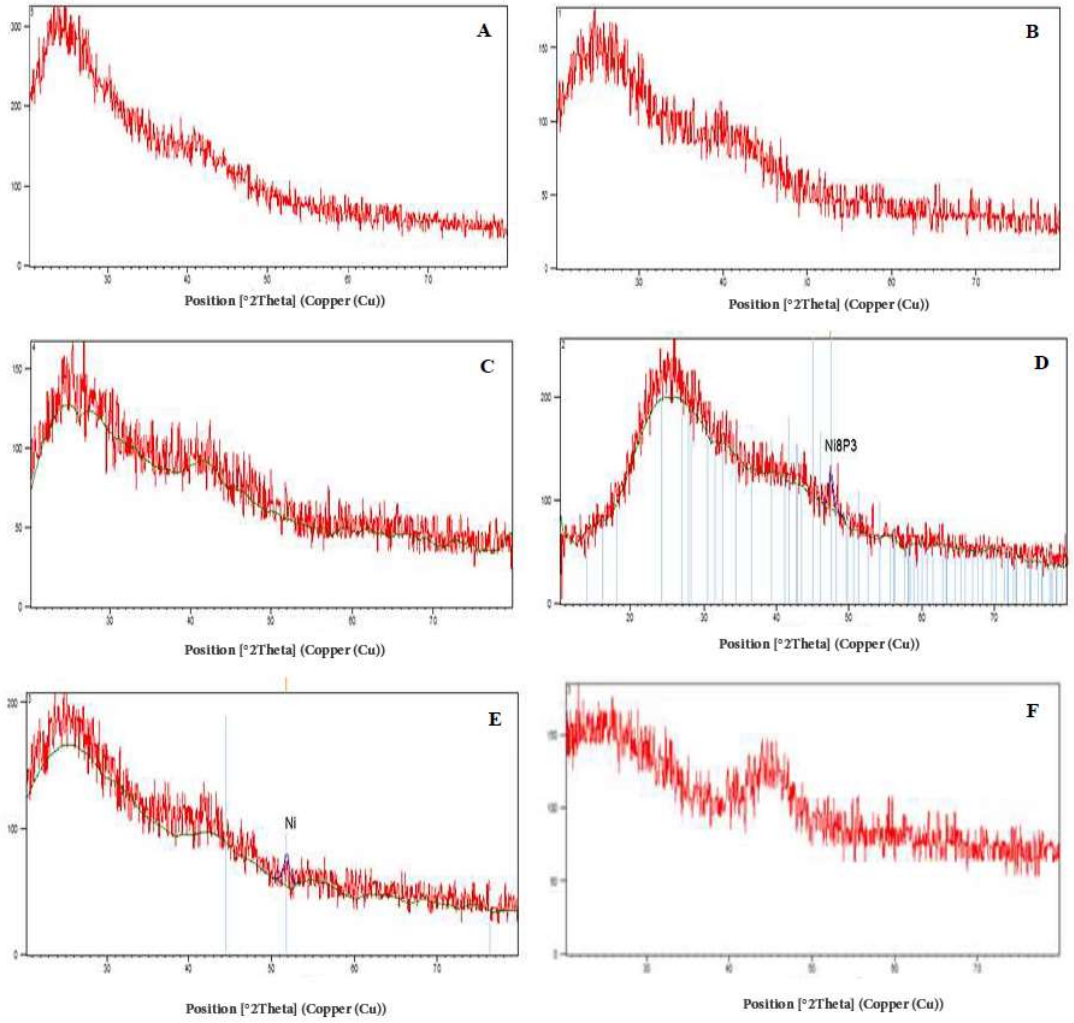

Fig. 1- XRD patterns of (A) Sample 1: uncoated glass fibers; (B) Sample 2: Ni–P coated glass fibers without heat treatment; (C) Sample 3: Ni–P coated glass fibers heat-treated at 300 °C; (D) Sample 4: Ni–P coated glass fibers heat-treated at 370 °C; (E) Sample 5: Ni–P coated glass fibers heat-treated at 450 °C; (F) Sample 6: Ni–P coating heat-treated at 300 °C.

In Figure 2, all the above diffraction peaks are presented in a single graph for better comparison.

According to Figure 1-C, Sample 3 similar to the previous samples exhibits no identifiable diffraction peaks. This appears to be due to high noise levels, likely related to the characteristics of the sample. In practice, the onset of crystallization in the coating was expected in this sample. The absence of peaks may be attributed to two factors: (1st) the sample was in bulk form with an uneven surface, and (2nd) the analyzed structure was in coating form. Both factors likely prevented the acquisition of high-resolution data needed to reveal the expected crystallographic structure. As shown in Figure 1-D, the XRD pattern of Sample 4 reveals only a weak diffraction peak, which considering the previously mentioned sources of noise might indicate the initial stages of crystallization in the coating.

Similarly, Figure 1-E illustrates that Sample 5 does not display any distinguishable diffraction peaks, again due to the factors noted above. The XRD results for the detached and heat-treated coatings deposited on glass slides are as follows: Figure 1-F shows the XRD pattern of the Ni–P coating heat-treated at 300 °C. No characteristic peaks are observed, suggesting that crystallization had not yet begun. This may be due to the one-hour holding time at 300 °C being insufficient for crystallization, or potentially due to unfavorable sample conditions for XRD analysis such as the bulk form and lack of powder preparation despite previous studies indicating that this temperature marks the onset of crystallization [9, 12, 14].

According to Figure 3, the XRD pattern of the coating heat-treated at 370 °C exhibits characteristic peaks corresponding to Ni and Ni_3P phases, which were expected to form under the applied thermal treatment conditions [9, 21].

According to Figure 4, the XRD pattern of the coating heat-treated at 450 °C reveals characteristic peaks corresponding to Ni, $Ni_{12}P_5$, and Ni_3P phases, which were expected to form under the applied thermal treatment conditions [9, 14, 21]. In this case, the Ni_3P peak was anticipated to exhibit a relatively higher intensity compared to the same peak in the sample heat-treated at 370 °C [9]. Based on the Scherrer equation, the crystallite size of the Ni_3P phase was calculated for the samples heat-treated at both 370 °C and 450 °C as follows:

$$D = (0.9 * \lambda) / (\beta \cos\theta) \quad (1)$$

According to the XRD analysis, the crystallite size of the Ni_3P phase in the sample heat-treated at 450 °C was calculated to be 43.19 nm, while that in the sample heat-treated at 370 °C was 21.61 nm. This indicates a greater grain growth at the higher temperature, which is consistent with findings reported in similar studies [16, 21]. As the heat treatment temperature increases to 450 °C, the Ni_3P diffraction peak becomes significantly sharper and more intense, indicating enhanced crystallinity and thermally activated grain growth within the EN coating.

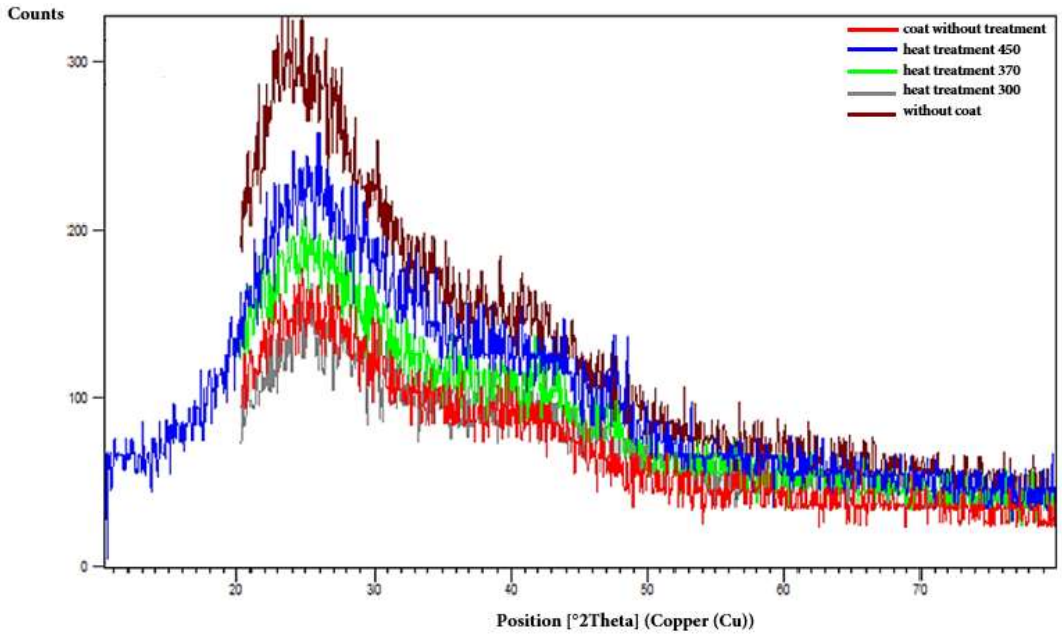

Fig. 2- XRD patterns of five fiber samples

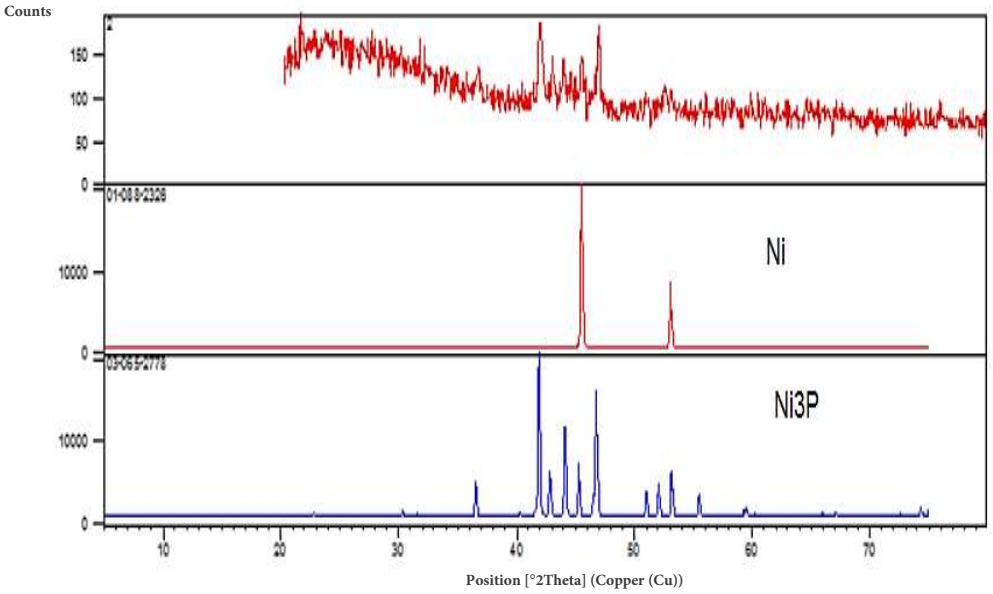

Fig. 3- XRD pattern of Sample 7 (Ni–P coating heat-treated at 370 °C), showing the peak positions of Ni and Ni_3P phases.

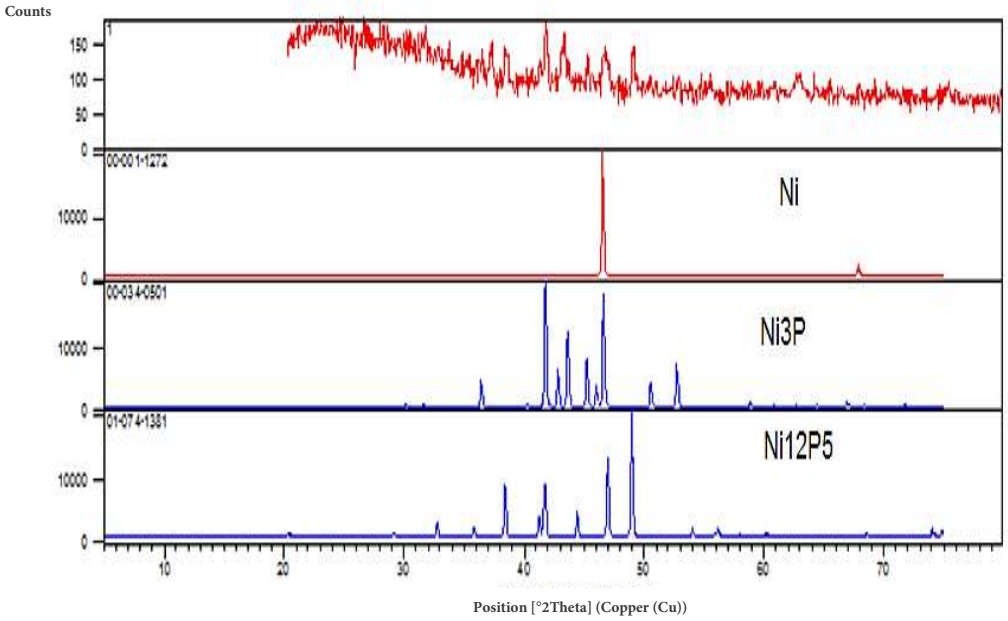

Fig. 4- XRD pattern of Sample 8 (Ni–P coating heat-treated at 450 °C), showing the peak positions of Ni, Ni_3P, and $Ni_{12}P_5$ phases.

Table 3- Characterization of Specimens Using FESEM

Sample No.	Sample Description
1	Glass fibers coated with EN, without heat treatment
2	Glass fibers coated with EN, heat treated at 300 °C
3	Glass fibers coated with EN, heat treated at 370 °C
4	Glass fibers coated with EN, heat treated at 450 °C
5	Thermal shock sample of glass fibers coated with EN, without heat treatment
6	Thermal shock sample of glass fibers coated with EN, heat treated at 300 °C
7	Thermal shock sample of glass fibers coated with EN, heat treated at 370 °C
8	Thermal shock sample of glass fibers coated with EN, heat treated at 450 °C
9	A356 aluminum matrix composite reinforced with EN-coated glass fibers, without heat treatment
10	A356 aluminum matrix composite reinforced with EN-coated glass fibers, heat treated at 300 °C
11	A356 aluminum matrix composite reinforced with EN-coated glass fibers, heat treated at 370 °C
12	A356 aluminum matrix composite reinforced with EN-coated glass fibers, heat treated at 450 °C

3.2. Analysis and Evaluation of Field Emission Scanning Electron Microscopy (FESEM) Images

As outlined in Table 3, the microstructural features of the examined specimens, analyzed via FESEM, are presented accordingly:

The heat treatment of electroless nickel (EN) coatings can lead to significant changes in their properties and microstructure. It is well established that heating EN deposits within the temperature range of 300 – 400 °C and maintaining them at that level for one hour enhances the hardness of the coating due to the formation of nickel phosphide phases. The heat treatment was conducted in a tube furnace under an inert argon atmosphere to prevent the formation of oxide layers. Following the heat treatment, samples were cooled in ambient air [21].

One of the primary objectives of heat treating EN coatings is to improve their adhesion to the substrate and enhance their overall stability [21]. This effect is well illustrated in the SEM images presented in the following section. Figure 5-A displays the EN-coated glass fibers without heat treatment, where a continuous Ni–P deposit is clearly visible on the surface. The white agglomerates observed may correspond to volatile compounds, which are no longer present in the heat-treated specimens. Figure 5-B, showing the EDS analysis of the EN-coated glass fibers without thermal treatment, reveals the elemental composition of the coating as well as the underlying substrate."

The quantitative EDS analysis presented in Table 4 reveals the elemental composition of the EN-coated glass fibers prior to heat treatment. Notably, the coating exhibits a significant presence of nickel and phosphorus, consistent with the formation of a Ni–P layer through the electroless plating process. This elemental distribution supports the observed morphology in Figure 5-A, where a continuous and uniform Ni–P deposit is evident on the glass fiber surface. Furthermore, the disappearance of white agglomerates in Figure 6-A corresponding to the sample heat-treated at 300 °C suggests that these features likely represent volatile residues that were effectively removed during the thermal process. This observation indicates that heat treatment not only alters the microstructural integrity of the coating but also enhances its purity and surface uniformity, which are critical factors in improving adhesion and functional performance.

As depicted in Figure 6-B, the average grain size of the EN coating on glass fibers heat treated at 300 °C is approximately 11.8 nm. This nanoscale refinement may influence both the hardness and structural homogeneity of the coating. Table 5 presents the quantitative EDS analysis of the same sample, revealing a reduction in the nickel and phosphorus content compared to the as-deposited coating. This decrease may be attributed either to the inherent limitations in the spatial resolution and accuracy of EDS or to the partial volatilization and migration of certain elements during heat treatment. Nevertheless, given the semiquantitative nature of EDS analysis, conclusive interpretations remain challenging. In Figure 7-A, the EN-coated glass fibers subjected to heat treatment at 370 °C display a more pronounced and distinguishable granular morphology. The coating particles are clearly visible and well-defined on the glass fiber surface, suggesting a substantial alteration in microstructure with increasing temperature.

Figure 7-C presents the EDS analysis results of EN-coated glass fibers subjected to heat treatment at 370 °C, indicating the presence of various elements associated with both the coating and the glass fiber substrate. As shown in Table 6, the quantitative EDS results reveal that the nickel and phosphorus content in the coating has not significantly changed compared to the sample heat-treated at 300 °C. However, due to the semiquantitative nature of EDS, a definitive interpretation cannot be made.

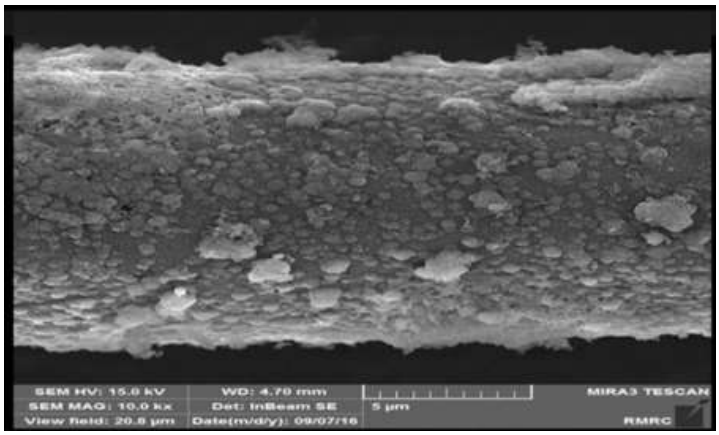

A

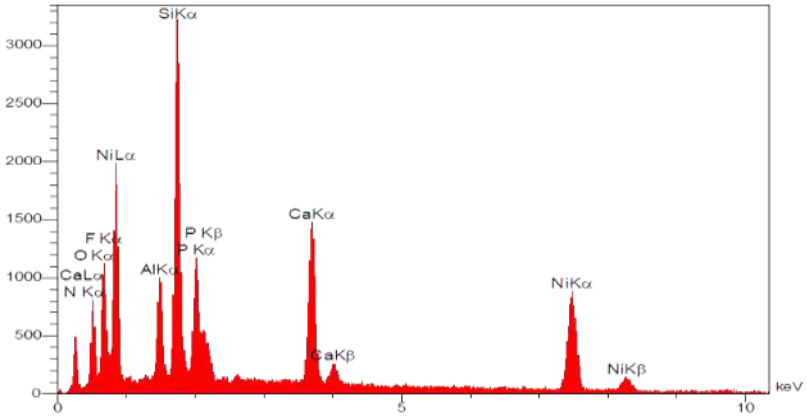

B

Fig. 5- (A) EN-coated glass fibers without heat treatment; (B) EDS spectrum of EN-coated glass fibers without heat treatment.

Table 4- Elemental Composition Obtained via EDS Analysis of Unheat-Treated EN-Coated Glass Fibers

Element (Symbol)	Line	Weight Percentage (W%)
Nitrogen (N)	Ka	1.33
Oxygen (O)	Ka	15.00
Fluorine (F)	Ka	13.31
Aluminum (Al)	Ka	3.64
Silicon (Si)	Ka	13.15
Phosphorus (P)	Ka	6.23
Calcium (Ca)	Ka	11.38
Nickel (Ni)	Ka	35.97

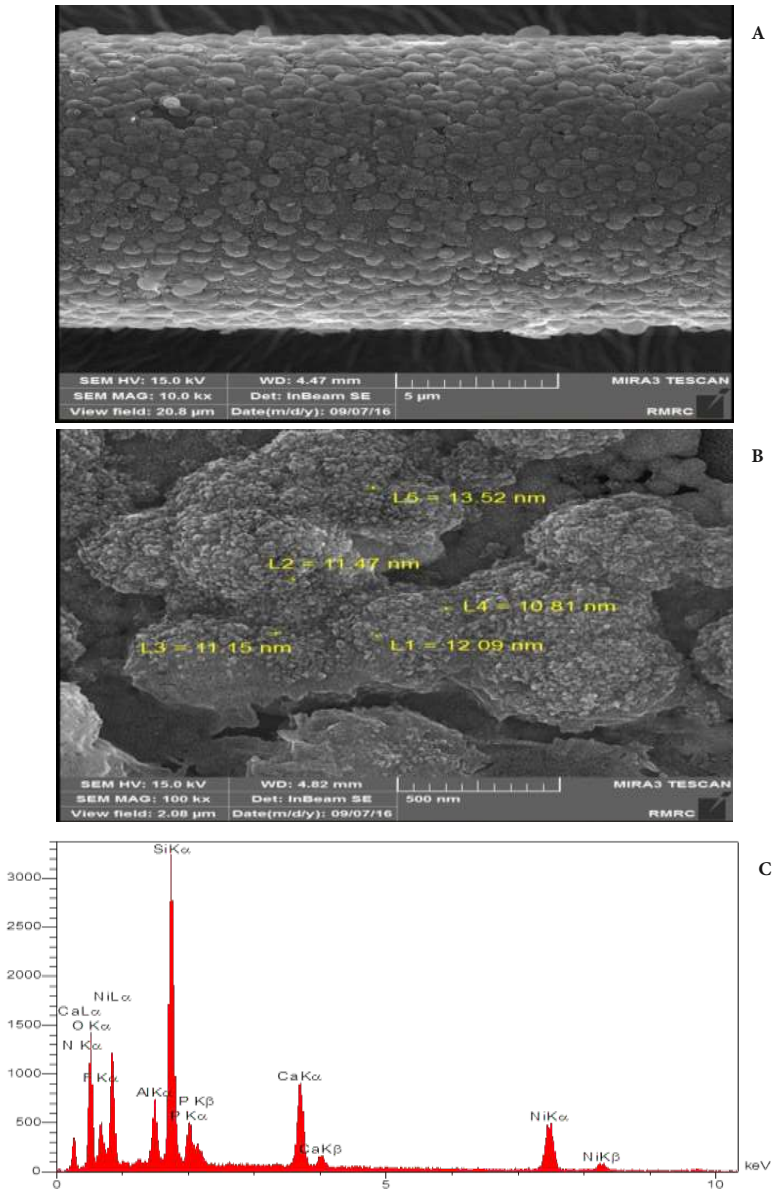

Fig. 6- (A) EN-coated glass fibers heat treated at 300 °C; (B) Grain size of the EN coating on glass fibers heat treated at 300 °C; (C) EDS spectrum of EN-coated glass fibers after heat treatment at 300 °C.

Table 5- Elemental Composition of EN-Coated Glass Fibers Following Heat Treatment at 300 °C (Based on EDS Analysis)

Element (Symbol)	Line	Weight Percentage (W%)
Nitrogen (N)	Ka	1.63
Oxygen (O)	Ka	29.80
Fluorine (F)	Ka	9.39
Aluminum (Al)	Ka	3.53
Silicon (Si)	Ka	16.79
Phosphorus (P)	Ka	3.32
Calcium (Ca)	Ka	9.00
Nickel (Ni)	Ka	26.53
Total	-	100

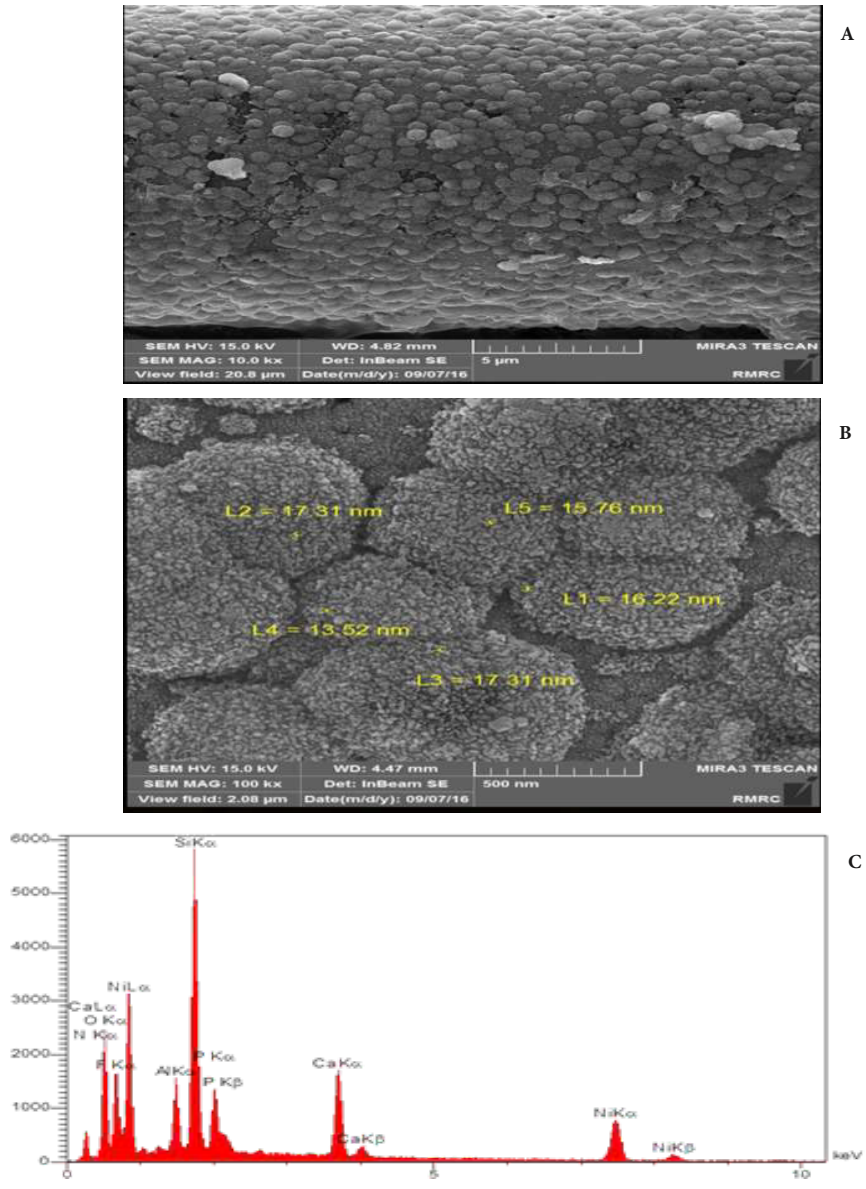

Fig. 7- (A) Scanning electron micrograph of EN-coated glass fibers subjected to heat treatment at 370 °C. (B) Grain size distribution of the EN coating on glass fibers after heat treatment at 370 °C. (C) Energy dispersive spectroscopy (EDS) spectrum of EN-coated glass fibers treated at 370 °C.

Table 6- Quantitative EDS analysis of EN-coated glass fibers after heat treatment at 370 °C

Element (Symbol)	Line	Weight Percentage (W%)
Nitrogen (N)	Ka	2.29
Oxygen (O)	Ka	27.13
Fluorine (F)	Ka	16.65
Aluminum (Al)	Ka	3.80
Silicon (Si)	Ka	15.14
Phosphorus (P)	Ka	4.77
Calcium (Ca)	Ka	8.39
Nickel (Ni)	Ka	21.84
Total	-	100

Figure 8-A displays the EN-coated glass fibers after heat treatment at 450 °C, where the preservation of coating particle integrity is clearly observable. This suggests that the deposited layer maintains its structural coherence despite the elevated thermal exposure.

Figure 8-B illustrates the grain size distribution of the EN coating on glass fibers heat treated at 450 °C. As observed, the average grain size reaches approximately 20.8 nm, indicating grain growth compared to the samples heat treated at 300 and 370 °C. This suggests that elevated thermal exposure enhances atomic mobility, promoting crystallite coarsening. A comparative evaluation of the FESEM-derived grain size data reveals a clear temperature-dependent growth trend. The average grain size increased from 11.8 nm at 300 °C to approximately 20.8 nm at 450 °C, corresponding to nearly a 76% increase in grain dimension. This grain coarsening behavior is consistent with the

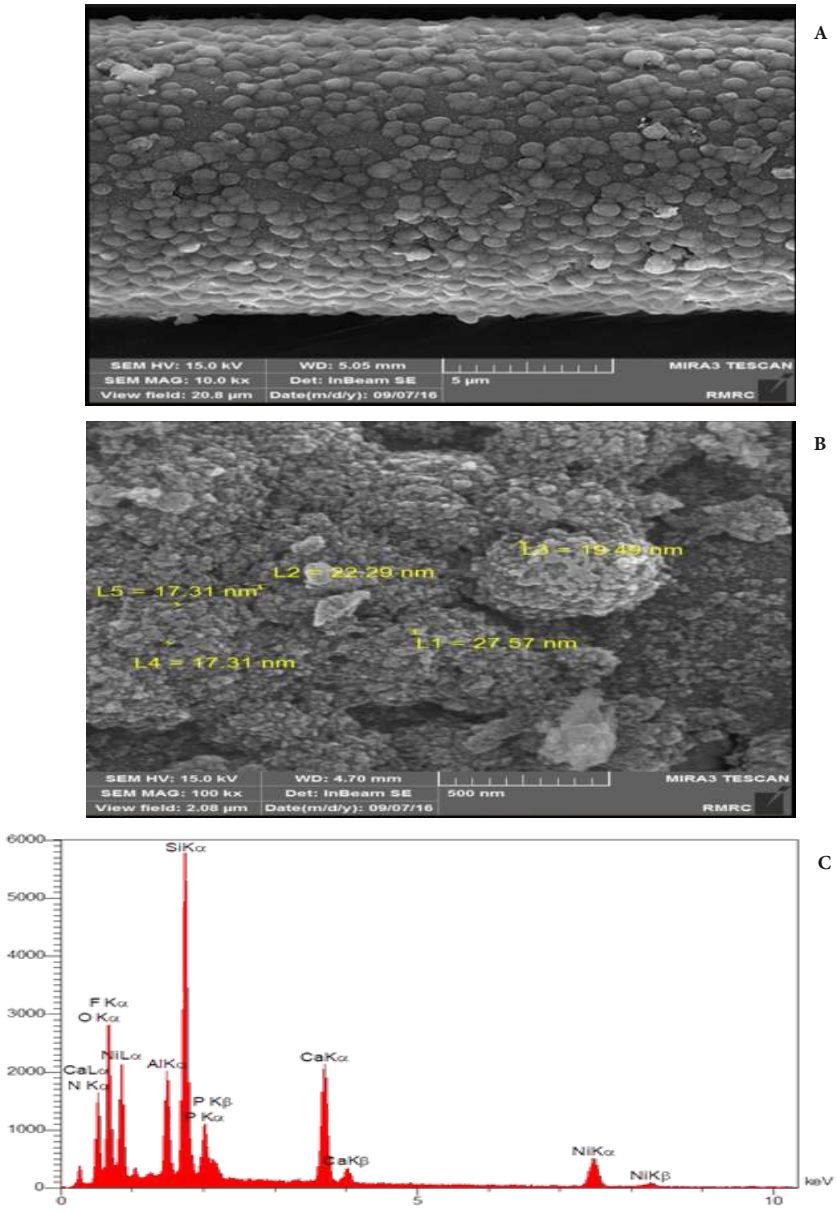

Fig. 8- (A) Scanning electron micrograph of EN-coated glass fibers subjected to heat treatment at 450 °C. (B) Grain size distribution of the EN coating on glass fibers after heat treatment at 450 °C. (C) Energy dispersive spectroscopy (EDS) spectrum of EN-coated glass fibers treated at 450 °C.

XRD-based crystallite size calculations, which showed an increase in Ni_3P crystallite size from 21.61 nm at 370 °C to 43.19 nm at 450 °C. The combined FESEM and XRD results confirm that heat treatment induces structural reorganization and crystallization within the EN coating. The formation and growth of crystalline Ni and Ni_3P phases contribute to improved coating stability, enhanced adhesion to the glass substrate, and superior performance during in-melt filament winding.

Figure 8-C presents the EDS spectrum of the same sample, confirming the presence of both coating elements and substrate constituents. According to the quantitative EDS results shown in Table 7, the nickel and phosphorus contents are lower than those in the coatings heat treated at 300 and 370 °C. This reduction may be attributed to the localized nature of EDS analysis and compositional variation at specific points on the fiber surface.

Table 7- Quantitative elemental analysis (EDS) of EN-coated glass fibers heat-treated at 450 °C

Element (Symbol)	Line	Weight Percentage (W%)
Nitrogen (N)	**Ka**	**1.78**
Oxygen (O)	**Ka**	**20.64**
Fluorine (F)	**Ka**	**27.73**
Aluminum (Al)	**Ka**	**5.22**
Silicon (Si)	**Ka**	**15.60**
Phosphorus (P)	**Ka**	**3.87**
Calcium (Ca)	**Ka**	**11.19**
Nickel (Ni)	**Ka**	**13.96**
Total	**-**	**100**

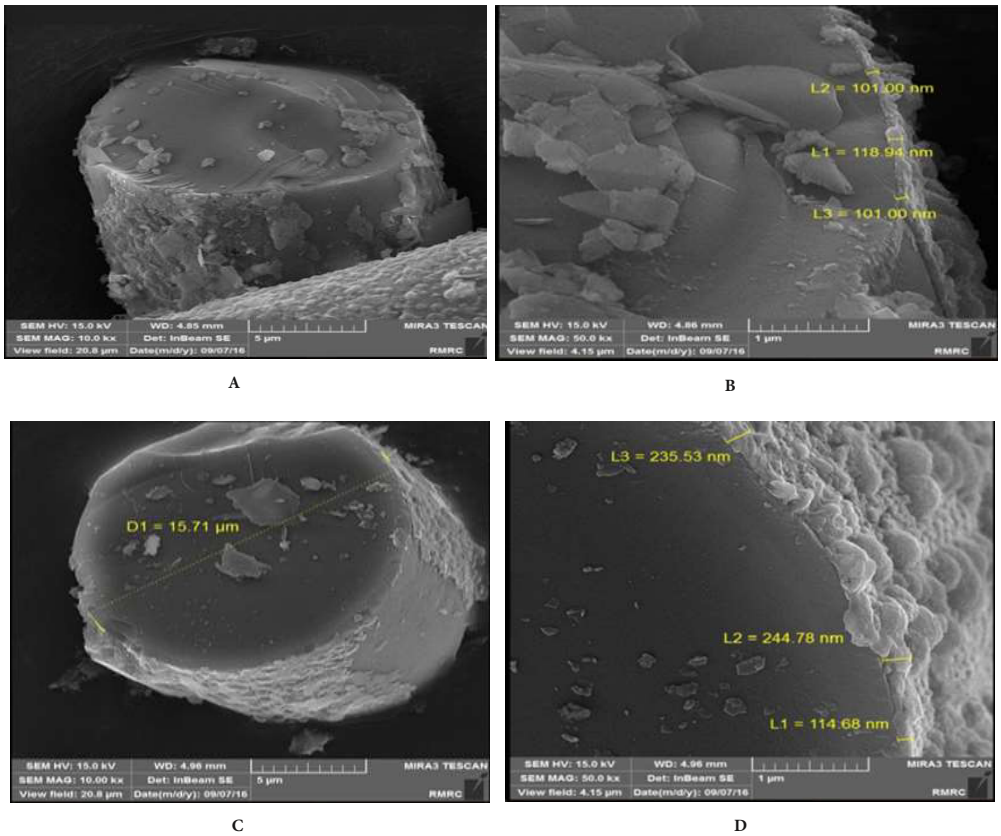

Fig. 9- (A) Cross-sectional micrograph of EN-coated glass fibers after heat treatment at 370 °C. (B) Coating thickness of EN layer on glass fibers heat-treated at 370 °C. (C) Cross-sectional micrograph of EN-coated glass fibers after heat treatment at 450 °C. (D) Coating thickness of EN layer on glass fibers heat-treated at 450 °C.

Comparative analysis of Figures 6-B, 7-B, and 8-B clearly reveals that the grain size of the EN coating increases with rising heat treatment temperature. This trend is corroborated by the Scherrer equation-based grain size estimations of Ni_3P phases obtained via XRD analysis. The elemental presence of phosphorus and nickel as the principal components of EN coatings is consistently confirmed across all EDS datasets. However, due to the penetration of the EDS beam into the underlying substrate, precise determination of the coating's composition remains challenging. Nonetheless, the data is still valuable for comparative interpretation."

Figure 9-A displays the cross-sectional view of EN-coated glass fibers after heat treatment at 370 °C, while Figure 9-B shows the corresponding coating thickness. Figure 9-C presents the cross-sectional image of EN-coated glass fibers heat treated at 450 °C, highlighting the fiber diameter. In Figure 9-D, the coating thickness for the 450 °C-treated sample is depicted. Due to the specimen's positioning angle in Figure 9-D, only the thickness value denoted as L1 = 114.68 nm can be considered reliable. Based on this assumption and by comparing Figures 9-B and 9-D it can be inferred that the heat treatment process does not cause a significant change in coating thickness.

3.3. FESEM Characterization of Thermally Shocked Samples

The following images display EN-coated glass fiber samples that were heat treated at various temperatures and subsequently subjected to thermal shock testing in accordance with ASTM Standard D6182-84, in order to evaluate the adhesion strength between the coating and the substrate. According to the standard, each sample was heated to 200 °C and then immediately quenched in water at ambient temperature (25 °C). This heating and cooling cycle was repeated eight times for each specimen.

As shown in Figure 10-A, the EN-coated glass fibers without heat treatment exhibited partial delamination of the coating at multiple locations along the fiber surface. This observation clearly indicates weak interfacial adhesion between the coating and the substrate in the as-deposited condition.

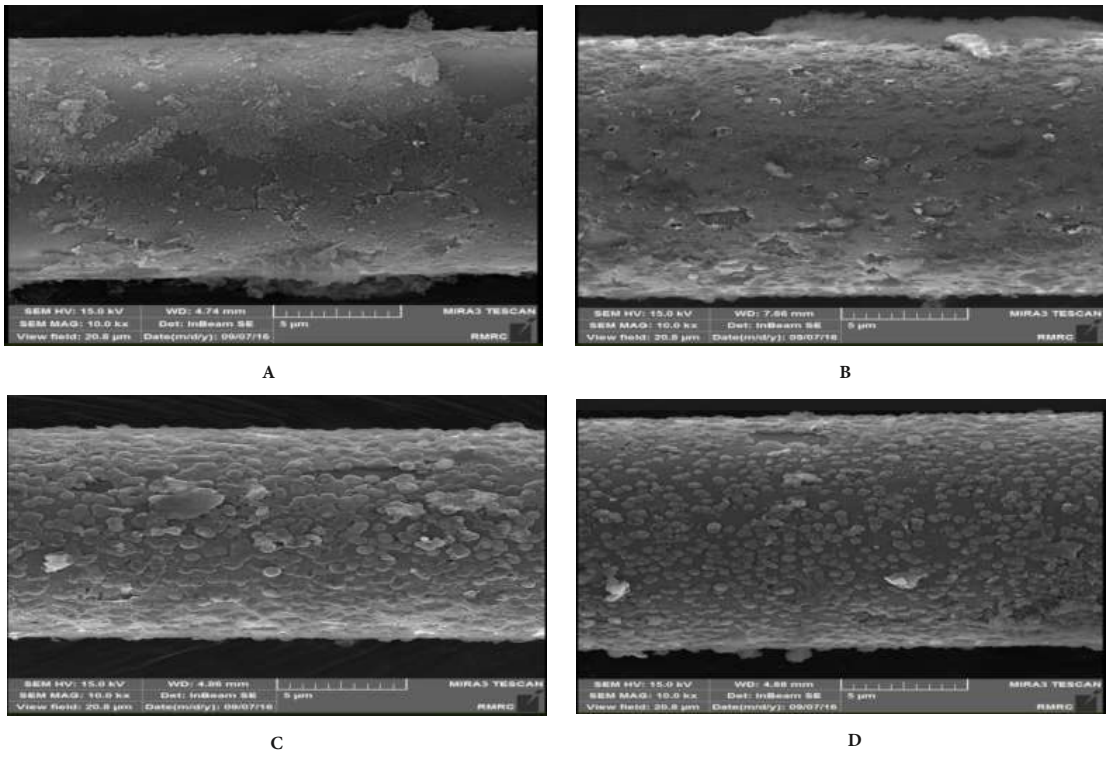

Fig. 10- (A) Thermal shock sample of EN-coated glass fibers without heat treatment. (B) Thermal shock sample of EN-coated glass fibers heat-treated at 300 °C. (C) Thermal shock sample of EN-coated glass fibers heat-treated at 370 °C. (D) Thermal shock sample of EN-coated glass fibers heat-treated at 450 °C

As shown in Figure 10-B, the EN-coated glass fibers heat treated at 300 °C exhibit minor voids and coating-deficient regions, though these imperfections are significantly fewer than those observed in the non-heat-treated specimens. This indicates that the heat treatment process improves the adhesion of the coating to the fiber substrate. In Figures 10-C and 10-D, corresponding to samples heat treated at 370 °C and 450 °C respectively, such voids and delaminated areas are rarely observed, further confirming that elevated thermal treatment enhances interfacial bonding between the EN coating and the substrate.

The primary purpose of coating the glass fibers was to improve their wettability with molten aluminum. During the fiber winding process into the aluminum melt, friction between the coated fibers and the molten metal can cause delamination of the EN coating if its adhesion to the fiber surface is insufficient. In such cases, the EN layer may easily detach and dissolve into the melt. The following figures illustrate the composite specimens fabricated via the molten aluminum fiber winding technique, with detailed descriptions of the fiber characteristics provided in the subsequent section.

3.4. FESEM Characterization of A356 Aluminum Matrix Composites Reinforced with EN-Coated Glass Fibers

a. EN-coated glass fibers without heat treatment
b. EN-coated glass fibers heat treated at 300 °C
c. EN-coated glass fibers heat treated at 370 °C
d. EN-coated glass fibers heat treated at 450 °C

A356 aluminum alloy was used as the matrix in the fiber winding process. In each of the four aforementioned images, the interfacial bonding between the glass fibers and the aluminum matrix, as well as the local matrix composition near the fiber–matrix interface, were evaluated using EDS analysis. As observed in the FESEM image shown in Figure 11-A, the coating particles are no longer distinctly visible after undergoing the fiber winding process. Based on the EDS results presented in Figure 11-B and Table 8, the matrix composition near the glass fiber surface contains approximately 10.51 wt.% nickel and 0.64 wt.% phosphorus. This elemental distribution indicates that portions of the EN coating detached from the fibers and were incorporated into the aluminum matrix. The inadequate adhesion of the EN coating in the non-heat-treated samples appears to be the primary cause of this phenomenon, as also confirmed by the thermal shock tests.

Due to the weak bonding between the coating and the fibers, it is unlikely that the aluminum melt would effectively adhere to the fibers during the winding process. Once the aluminum melt contacts the EN coating, especially under turbulent flow and frictional forces, the lack of strong interfacial bonding results in separation of the coating, which then becomes dispersed within the melt. This behavior is further confirmed by the EDS data in Table 8. The subsequent images illustrate fiber-wound composite samples containing EN-coated fibers that were heat treated at 300 °C, 370 °C, and 450 °C. These are compared with the aforementioned results to clearly demonstrate the beneficial role of heat treatment in enhancing coating integrity and fiber–matrix interfacial performance.

Table 8 presents the quantitative EDS results of the matrix composition near the fibers in the A356 aluminum matrix composite reinforced with electroless nickel–phosphorus (Ni–P) coated glass fibers without heat treatment.

Figure 12-A shows the FESEM image of an A356 aluminum matrix composite reinforced with EN-coated glass fibers heat treated at 300 °C. The image illustrates the embedding of the glass fibers within the aluminum matrix and demonstrates the interfacial bonding between the fibers and the matrix. Figure 12-B shows the FESEM image of an A356 aluminum matrix composite reinforced with EN-coated glass fibers heat treated at 300 °C. An EDS analysis was performed on the aluminum matrix near the fiber–matrix interface, as indicated by the marked region in this image. The corresponding results are presented in Figures 12-C and Table 9. The image clearly demonstrates strong interfacial bonding between the aluminum matrix and the heat-treated, EN-coated glass fibers.

According to Table 9 and based on the measured nickel and phosphorus content in the matrix adjacent to the fibers, it is evident that the coating did not detach from the fibers to the same extent as observed in the non-heat-treated sample. This indicates improved interfacial adhesion between the coating and the fibers as a result of the heat treatment.

Figure 13-A shows the FESEM image of the A356 aluminum matrix composite reinforced with EN-coated glass fibers heat treated at 370 °C. An EDS analysis was conducted on the aluminum matrix near the fiber–matrix interface, as indicated in the marked region of the image, and the results are presented in Figure 13-B.

According to Table 10, which displays the EDS results of the aluminum matrix near the fibers in the same composite, the nickel content in the matrix is significantly lower than that observed in the composite reinforced with non-heat-treated coated fibers. This substantial difference indicates that the EN coating remained more firmly attached to the fibers in the heat-treated sample, demonstrating improved interfacial adhesion as a result of the thermal treatment.

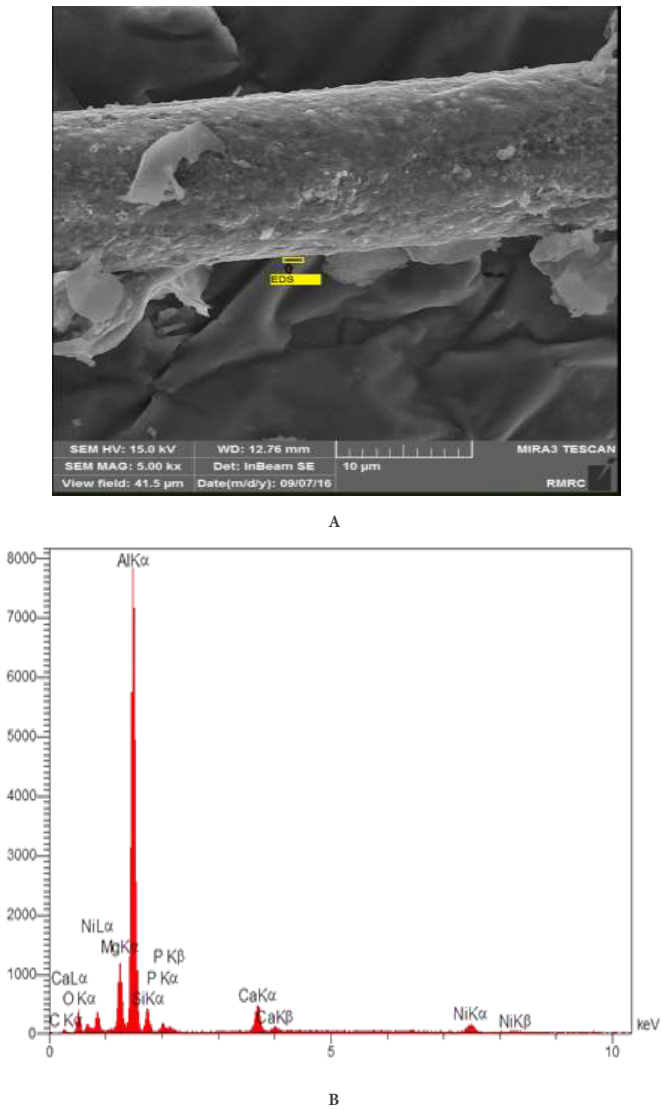

Fig. 11- (A) Field Emission Scanning Electron Microscopy (FESEM) image of A356 aluminum matrix composite reinforced with EN-coated glass fibers without heat treatment. (B) Energy Dispersive Spectroscopy (EDS) spectrum of the aluminum matrix near the fibers in the A356 aluminum matrix composite reinforced with EN-coated glass fibers without heat treatment.

Table 8- Quantitative EDS analysis of the aluminum matrix near the EN-coated glass fibers in the A356 composite without heat treatment

Element (Symbol)	Line	Weight Percentage (W%)
Carbon (C)	Ka	10.79
Oxygen (O)	Ka	12.72
Magnesium (Mg)	Ka	6.66
Aluminum (Al)	Ka	50.28
Silicon (Si)	Ka	2.80
Phosphorus (P)	Ka	0.64
Calcium (Ca)	Ka	5.60
Nickel (Ni)	Ka	10.51
Total	-	100

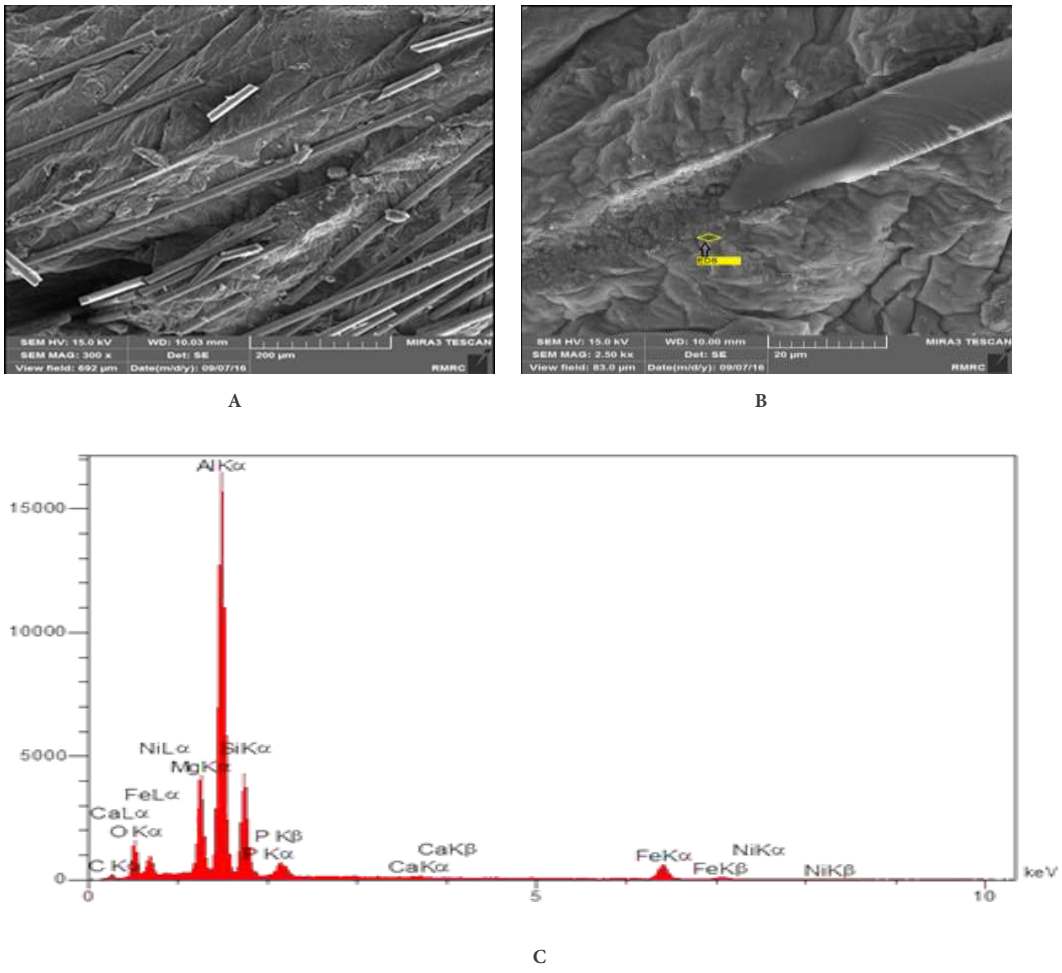

Fig. 12-(A,B) Field Emission Scanning Electron Microscopy (FESEM) images of the A356 aluminum matrix composite reinforced with EN-coated glass fibers after heat treatment at 300 °C. (C) Energy Dispersive Spectroscopy (EDS) spectrum of the aluminum matrix near the EN-coated glass fibers in the A356 composite after heat treatment at 300 °C.

Table 9- Quantitative EDS analysis of the aluminum matrix near the EN-coated glass fibers in the A356 composite after heat treatment at 300 °C

Element (Symbol)	Line	Weight Percentage (W%)
Carbon (C)	Ka	12.63
Oxygen (O)	Ka	17.48
Magnesium (Mg)	Ka	9.13
Aluminum (Al)	Ka	38.30
Silicon (Si)	Ka	12.61
Phosphorus (P)	Ka	0.51
Calcium (Ca)	Ka	0.33
Iron (Fe)	Ka	8.90
Nickel (Ni)	Ka	0.11
Total	-	100

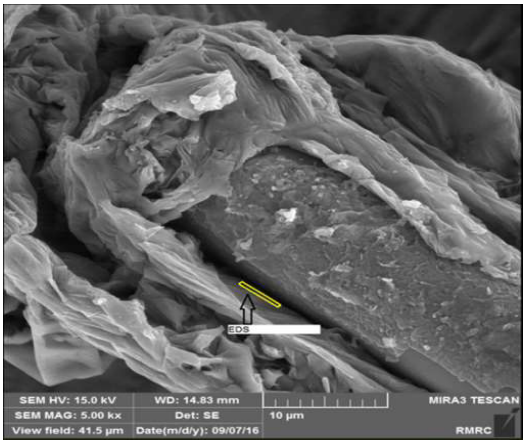

A

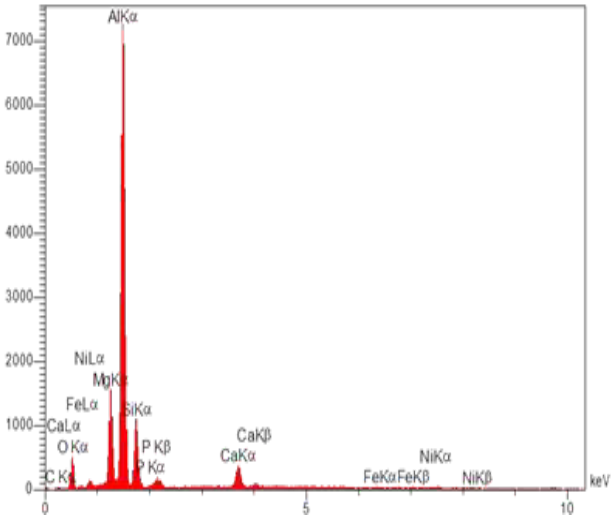

B

Fig. 13- (A) Field Emission Scanning Electron Microscopy (FESEM) image of the A356 aluminum matrix composite reinforced with EN-coated glass fibers after heat treatment at 370 °C. (B) Energy Dispersive Spectroscopy (EDS) spectrum of the aluminum matrix near the EN-coated glass fibers in the A356 composite after heat treatment at 370 °C.

Table 10- Quantitative EDS analysis of the aluminum matrix near the EN-coated glass fibers in the A356 composite after heat treatment at 370 °C

Element (Symbol)	Line	Weight Percentage (W%)
Carbon (C)	Ka	7.23
Oxygen (O)	Ka	18.24
Magnesium (Mg)	Ka	8.96
Aluminum (Al)	Ka	49.22
Silicon (Si)	Ka	9.82
Phosphorus (P)	Ka	0.05
Calcium (Ca)	Ka	4.78
Iron (Fe)	Ka	0.40
Nickel (Ni)	Ka	1.29
Total	-	100

Figure 14-A shows the FESEM image of an A356 aluminum matrix composite reinforced with EN-coated glass fibers heat treated at 450 °C. The location where EDS was performed on the aluminum matrix near the glass fibers is indicated. The image clearly demonstrates strong interfacial bonding between the matrix and the fibers, which can be attributed to the thermally treated electroless nickel–phosphorus coating.

Figure 14-B presents the EDS spectrum of the aluminum matrix near the glass fibers in the A356 aluminum matrix composite reinforced with EN-coated fibers heat treated at 450 °C, highlighting the elemental composition of the matrix at the fiber interface. Table 11 displays the corresponding quantitative EDS results. Similar to the trends observed in the composites reinforced with EN-coated fibers heat treated at 300 °C and 370 °C, no significant detachment of the coating into the matrix is evident in this specimen either. This further confirms the improved adhesion of the EN coating to the glass fibers as a result of the 450 °C heat treatment.

Among the FESEM images of the three heat-treated fiber-reinforced composites, the most stable and continuous coating–fiber interface is observed in the sample treated at 450 °C. In contrast to the non-heat-treated composite where notable amounts of nickel and phosphorus were detected in the matrix adjacent to the fibers, the EDS analyses of the three thermally treated samples reveal no such elevated concentrations, indicating minimal coating detachment.

Furthermore, the improved melt adhesion to the EN-coated fibers in the 300 °C and 450 °C samples is clearly visible in the micrographs. This enhanced wettability is attributed, firstly, to the improved surface energy imparted by the EN coating and, secondly, to the strong interfacial bonding between the coating and the fiber, both of which are promoted by appropriate thermal treatment.

3.5. Results of Differential Scanning Calorimetry (DSC) Analysis

According to Table 12, DSC tests were performed on four samples from room temperature up to 720 °C under ambient atmosphere at a heating rate of 15 °C/min. Conducting DSC analyses in ambient atmosphere is uncommon, as these tests are typically carried out in an inert atmosphere to investigate crystallization behavior during heat treatment. In this study, however, the purpose of the DSC test was not to monitor the crystallization process of the coating, but rather to assess changes in the fibers and coating under practical application conditions, specifically simulating the fiber winding process at elevated temperatures in ambient atmosphere.

The DSC results of the samples listed in Table 13 are presented. According to the DSC thermogram shown in Figure 15-A, an endothermic peak is observed in the temperature range of 170–205 °C. Based on the composition of E-glass fibers provided in Table 13, this peak cannot be attributed to the decomposition of the fiber's main constituents. Instead, it is likely associated with the release of volatile components originating from the sizing material applied to the fibers or the evaporation of moisture absorbed over time.

Furthermore, Table 13 presents the chemical composition of the E-glass fibers before and after heat treatment up to 500 °C. The observed increase in mass near Tg may be attributed to oxidation processes, leading to an increase in oxygen content within the fibers.

From a thermodynamic perspective, the non-heat-treated EN coating is unstable, and its components are prone to react either with each other or with the surrounding atmosphere particularly at elevated temperatures. According to the DSC thermogram of the uncoated EN layer shown in Figure 15-B, two endothermic peaks are observed in the temperature ranges of 241–243 °C and 504–509 °C. The first peak is likely associated with the release of volatile substances such as fluorine, as suggested by the EDS quantitative results in which fluorine content is notably present in the coating composition. Furthermore, based on a previously published study on the oxidation behavior of EN coatings in air, it was reported that the oxidation reaction below 200 °C follows a logarithmic trend, with the oxide layer thickness increasing from approximately 6 Å at room temperature to about 15 Å at 200 °C [23].

At 300 °C, the reaction progresses slowly toward a parabolic oxidation regime, forming a layered structure in the oxidation products an outer layer of $Ni(OH)_2$ and an inner layer of nickel phosphate. In the intermediate region between these layers, the hydroxide gradually releases water and converts to NiO. As such, at 300 °C, water, $Ni(OH)_2$, and NiO are present simultaneously, with the formation of NiO occurring between the hydroxide and nickel phosphate phases [23]. The thermal peak around 500 °C may correspond to severe oxidation and the complete evaporation of hydroxide at that temperature. The observed 12.2% weight loss near Tg is likely associated with the rapid release of water (from hydroxide decomposition), providing further evidence for the thermal instability of the non-heat-treated coating at elevated temperatures.

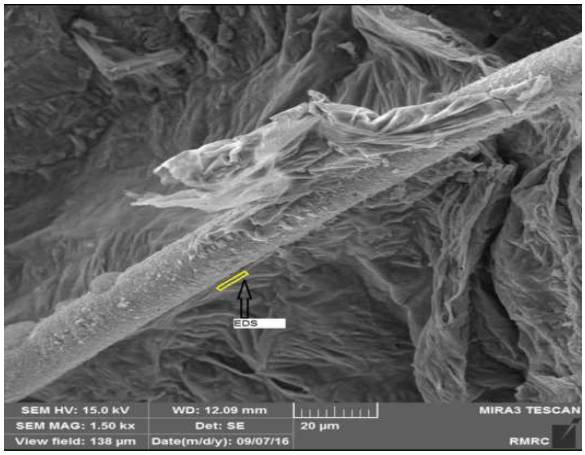

A

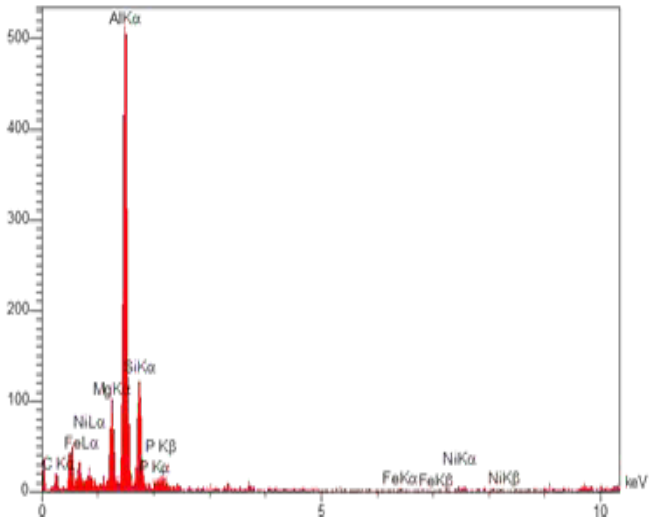

B

Fig. 14- (A) Field Emission Scanning Electron Microscopy (FESEM) image of the A356 aluminum matrix composite reinforced with EN-coated glass fibers after heat treatment at 450 °C. (B) Energy Dispersive Spectroscopy (EDS) spectrum of the aluminum matrix near the EN-coated glass fibers in the A356 composite after heat treatment at 450 °C.

Table 11- Quantitative EDS analysis of the aluminum matrix near the EN-coated glass fibers in the A356 composite after heat treatment at 450 °C

Element (Symbol)	Line	Weight Percentage (W%)
Carbon (C)	**Ka**	**45.64**
Magnesium (Mg)	**Ka**	**1.67**
Aluminum (Al)	**Ka**	**39.05**
Silicon (Si)	**Ka**	**9.67**
Phosphorus (P)	**Ka**	**0.22**
Iron (Fe)	**Ka**	**1.46**
Nickel (Ni)	**Ka**	**2.29**
Total	-	**100**

Table 12- DSC Test Samples

Sample Number	Sample Description
1	Uncoated glass fibers
2	EN coating without heat treatment
3	EN coating heat treated at 370 °C
4	EN coating heat treated at 450 °C

Table 13- Chemical Composition of E-Glass Fibers Before and After Heat Treatment up to 500 °C, Determined by EDX Analysis [22]

Fiber	O(%)		Na(%)		Al(%)		Si(%)		Ca(%)		Mg(%)	
	Min	Max	Min	Max	Min	Max	Min	Max	Min	Max	Min	Max
As- received	47.1	47.6	1.13	1.15	7.22	7.37	27.9	28.2	16.0	16.0	0.14	0.15
Heat treated	46.8	48.46	1.07	1.18	7.38	7.53	27.18	28.05	15.70	16.21	0.15	0.26

According to the DSC results shown in Figure 15-C for the EN-coated sample heat treated at 370 °C, two thermal peaks appear below 300 °C. Considering that the sample had already undergone prior heat treatment at 370 °C and that a 3% mass increase is observed near Tg, these peaks are unlikely to be associated with the release of volatile substances. Instead, they may be attributed to minor contamination of the samples prior to testing, given the extremely small sample mass (on the order of milligrams) used in the DSC analysis. The 3% mass gain observed in this specimen may be linked to oxygen uptake due to oxidation of certain coating constituents, such as nickel. According to the DSC curve in Figure 15-D for the EN-coated sample heat treated at 450 °C, no thermal peaks are observed. Additionally, the mass change indicated by Tg is negligible. These observations point to the high thermal stability of this sample, which can be attributed to the transformation of the coating structure from amorphous to crystalline, particularly involving the rearrangement of phosphorus and nickel atoms [21]. Considering this thermal stability under ambient atmospheric conditions as well as the field emission scanning electron microscopy (FESEM) results, which showed the highest degree of coating integrity and fiber–matrix adhesion at 450 °C , it can be concluded that the EN coating heat treated at 450 °C is the most suitable candidate for fiber winding in molten aluminum.

It is important to note that the mechanical strength of glass fibers decreases significantly at elevated temperatures due to two primary factors: (1) surface viscous flow and (2) structural rearrangement of the glass network. Therefore, glass fibers are not ideal for achieving high-strength performance under such conditions. Nonetheless, they were selected in this study because of their thermal stability in ambient atmosphere and chemical compatibility with both the electroless nickel (EN) coating and molten aluminum.

The most suitable reinforcement candidate for fiber winding in molten metals would be ceramic fibers from the Nextel family. However, despite considerable efforts, sourcing these fibers domestically was not feasible. It is worth noting that even with ceramic fibers, their poor wettability with metal melts necessitates fiber surface modification. Therefore, the findings of this research regarding fiber coating strategies can also be extended to ceramic fibers.

3.6. Evaluation of Fiber Winding Performance in Molten Metal Under Different Processing Conditions

Fiber winding into molten aluminum was performed under the following conditions:

a. Winding of uncoated fibers into pure molten aluminum at various temperatures

b. Winding of EN-coated glass fibers (without heat treatment) into pure molten aluminum.

c. Winding of EN-coated glass fibers (heat treated at 450 °C) into pure molten aluminum.

d. Winding of EN-coated fibers (without heat treatment) into A356 aluminum alloy melt at various temperatures.

e. Winding of EN-coated fibers (heat treated at 300 °C) into A356 aluminum alloy melt.

f. Winding of EN-coated fibers (heat treated at 370 °C) into A356 aluminum alloy melt.

g. Winding of EN-coated fibers (heat treated at 450 °C) into A356 aluminum alloy melt.

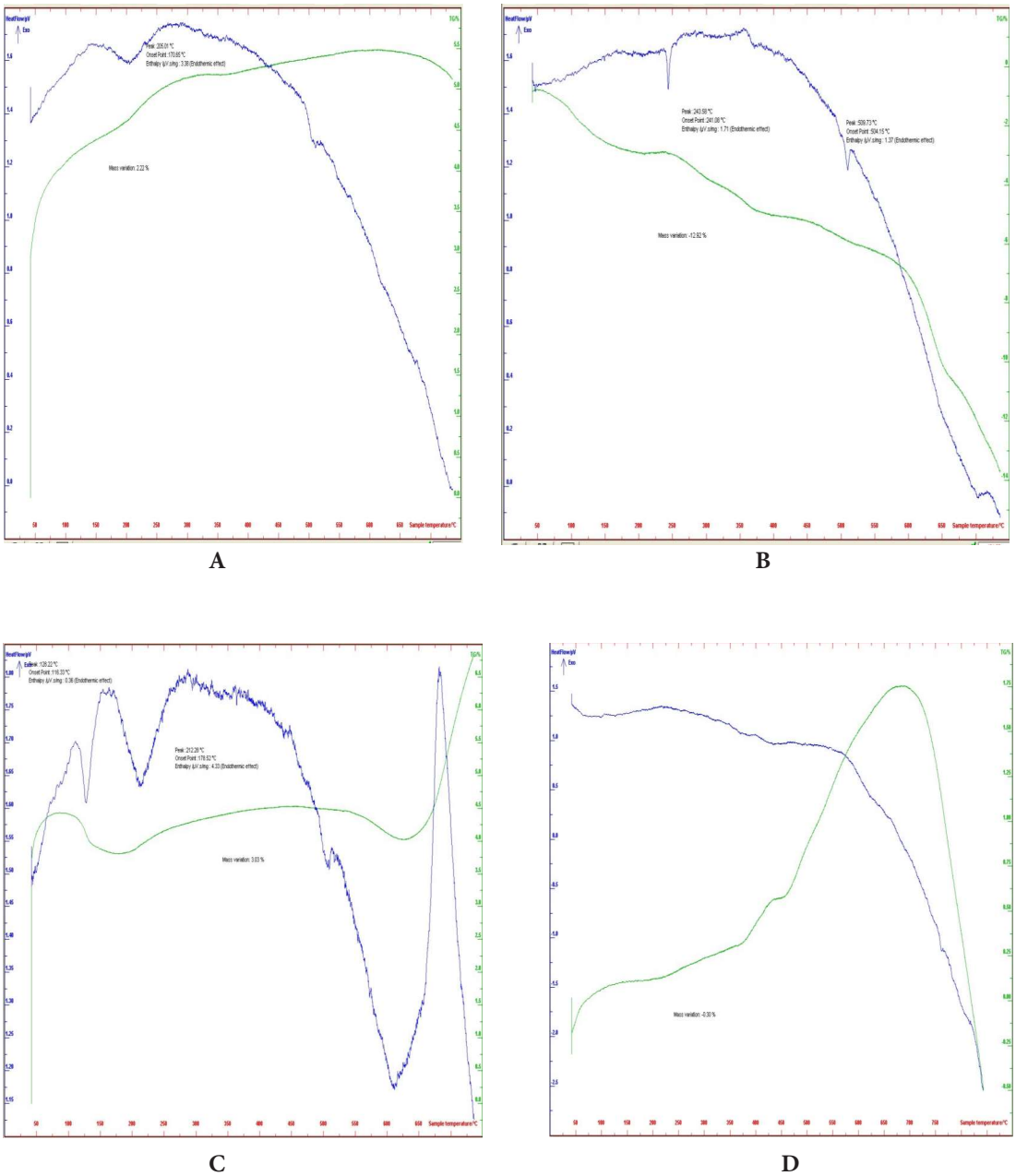

Fig. 15- (A) Differential Scanning Calorimetry (DSC) curve of uncoated glass fiber sample. (B) DSC curve of electroless nickel (EN) coating without heat treatment. (C) DSC curve of EN coating after heat treatment at 370 °C. (D) DSC curve of EN coating after heat treatment at 450 °C.

For condition 1, fiber winding was carried out at three temperatures: 820 °C, 770 °C, and 720 °C. Due to the weak wettability between the fibers and molten aluminum, as well as the low viscosity of the melt, the sample processed at 820 °C failed to form properly, with only slag adhering to the mandrel. In the sample wound at 770 °C, partial fiber embedding occurred, and aluminum filled the spaces between the fibers with a thin layer; however, fiber–aluminum separation was clearly observed due to poor wettability. In the sample processed at 720 °C, the thickness of the resulting tube was slightly greater than that at 770 °C, but fiber protrusion and inadequate wettability were also evident in this case. Based on the aforementioned tests, the optimal temperature for fiber winding in pure molten aluminum was determined to be 720 °C. At this temperature, the melt partially enters a semi-solid state, allowing the fibers to become embedded more effectively. As a result, subsequent fiber winding experiments in pure aluminum were conducted at 720 °C. In the case of Sample 2 where EN-coated glass fibers without heat treatment were used for winding in molten pure aluminum, the coating was observed to degrade immediately upon fiber immersion into the melt. Consequently, the winding process could not proceed.

In Sample 3, which involved fiber winding into pure molten aluminum using EN-coated glass fibers that were heat treated at 450 °C, with winding conducted at 720 °C, the best overall result was achieved across the entire study. Although the manual guidance of fibers onto the mandrel resulted in a non-uniform geometry, the embedding of fibers within the aluminum matrix, the filling of inter-fiber spaces, and the strong adhesion between the fibers and aluminum were all found to be satisfactory. “In the following four samples, fiber winding was performed in A356 aluminum alloy, and microstructural analysis was extensively conducted using FESEM imaging and EDS elemental mapping. Given that the solidification temperature of this alloy differs from that of pure aluminum, the fiber winding temperature also required adjustment specifically, to a lower value than that used for pure aluminum. Furthermore, due to the presence of silicon in the alloy and its high fluidity in the molten state, embedding of fibers within the melt proved challenging, resulting in incomplete or defective fiber winding. Therefore, achieving the desired outcome in molten aluminum fiber winding is unlikely in alloys that do not exhibit sufficiently high melt viscosity near their solidus temperature.

4. Conclusions

Key Findings from the Study on the Fabrication of Glass Fiber-Reinforced Aluminum Matrix Composite Tubes:

-One of the primary challenges in fabricating glass fiber-reinforced aluminum matrix composite tubes is the poor wettability between the fibers and molten aluminum.

-To address this issue, electroless nickel–phosphorus (Ni–P) coating was applied to E-glass fibers. The optimal coating was achieved using an acidic electroless bath formulation described in Table 5-1, with a final bath pH of 4–5 and an operating temperature of 90 °C.

-To improve the adhesion and stability of the coating on the fibers, heat treatment was applied at three temperatures: 300 °C, 370 °C, and 450 °C.

-Initial evaluation of the heat-treated EN coating on fibers was conducted via XRD analysis. However, due to poor sample condition and high noise, results were inconclusive. Therefore, XRD was repeated on a heat-treated EN coating deposited on a glass slide, which provided a smooth surface with similar composition to the actual fibers. The refined XRD data confirmed the formation of crystalline phases such as Ni, Ni_3P, and $Ni_{12}P_5$. Crystallite growth with increasing heat-treatment temperature was also evident, as estimated using the Scherrer equation.

-Field Emission Scanning Electron Microscopy (FESEM) was used to analyze the coating morphology. The micrographs demonstrated grain growth in the EN coating with increasing heat-treatment temperature. Elemental composition was further evaluated using EDS, which provided approximate concentrations of nickel and phosphorus.

-The adhesion between the EN coating and glass fibers was assessed via thermal shock testing according to ASTM E84. FESEM inspection after testing confirmed that the best adhesion occurred in the sample heat treated at 450 °C.

-DSC analysis was performed from room temperature up to 720 °C at a heating rate of 15 °C/min for four samples: (1) uncoated glass fibers, (2) EN-coated fibers without heat treatment, (3) EN-coated fibers heat treated at 370 °C, and (4) EN-coated fibers heat treated at 450 °C. The results indicated that the 450 °C heat-treated sample exhibited the highest thermal stability under ambient atmosphere.

-Glass fibers treated at 300 °C, 370 °C, and 450 °C, as well as fibers coated without heat treatment, were subjected to in-melt winding in A356 aluminum alloy. Surface morphology and adhesion were evaluated using FESEM, while EDS was used to examine the matrix composition near the fibers. The results indicated that in the non-heat-treated coated fibers, adhesion was poor and the EN coating detached from the fiber and bonded instead to the aluminum matrix.

-It was concluded that the most suitable aluminum for in-melt fiber winding is either pure aluminum or aluminum alloys that exhibit higher viscosity just before solidification. For pure aluminum, the optimal fiber-winding temperature was determined to be 720 °C.
-Overall, the results demonstrated that the electroless nickel (EN) coating heat treated at 450 °C provided the best performance for in-melt fiber winding in aluminum.

References

1. K. H. Krishman, S. John, K.N. Srinivasan, J. Ppraveen,M. Ganesan, and P.M. Kavimani, An Overall Aspect of Electroless Ni-P Depositions—A Review Article, Metallurgical and Materials Transactions A, Vacuum, 37(2006), 1917-1926.
2. S Kundu, S Kalyan, D and P Sahoo, Properties of electroless nickel at elevated temperature-a review, 12th global congress on manufacturing and management, 97(2014), 1698-1706, india.
3. H.Ying, H.Fei, Z. Wentao, S. Ke, Z. Li, W. Yanli, the study of electroless Ni-W-P alloy plating on glass fiber, Rare Metals, p.365, 2007.
4. B J.Kim, W K. Choi, H S. Song, J K. Park, J Y. Lee, S J. Park, preparation characterization of highly conductive nickel coated glass fibers, Carbon Latters,105-107, 2008.
5. Y. Jin, L. Hua, preparation and tribological properties of Ni-P electroless composite coating containing potassium titanate whisker, J.Mater Sci, china, 2007.
6. A. Daoud, Microstructure and tensile properties of 2014 Al alloy reinforced with continuous carbon fibers manufactured by gas pressure infiltration, Materials science and engineering, 1140120, 2005.
7. J. Zhang, S. Liu, Y. Zhang, Y. Dong, Y.Lu , T.Li , Fabrication of woven carbon fibers reinforced Al–Mg (95–5 wt%) matrix composites by an electromagnetic casting process, Journal of Materials Processing Technology, 78–84, 2015.
8. K. Zangeneh Madar, S. M. Monir Vaghefi, The effect of nitriding treatment on the structure, surface hardness and wear behavior of electroless Ni-P coated 4140 steel, Advanced Materials in Engineering, 23(2) (2022), 185-195.
9. K.G. Keong, W.Sha, crystallization and phase transformation behavior of electroless nickel-phosphorus deposites and their engineering properties, Material Literature, 329-343, 2002.
10. M.M Younan, I.H.M.Aly, M.T. Nageeb, effect of heat treatment on electroless ternary nickel-cobalt-phosphorus alloy, Journal of Applied Electrochemistry, 439-446, 2002.
11. K.G.Keong, W.Sha, S.Malinov, crystallization and phase transformation behavior of electroless nickel-phosphorus deposits with low and medium phosphorus contents under continuous heating, Journal of Materials Science, 37, 4445-4450, 2002.
12. S.H. Park, D.N.Lee, a study on the microstructure and phase transformation of electroless nickel deposits, Journal of Materials Science,1643-1654, Korea, 1988.
13. M.NOVAK, D.Vojtech, T. Vitu, influence of heat treatment on tribological properties of electroless Ni-P and Ni-Al2O3-P coating on Al-Si alloy, Prague, 2956-2960, 2010.
14. G.Jiaqiang, W.Yating, L.Lei, S.Bin, H.Wenbin, crystallization temperature of amorphous electroless nickel-phosphorus alloy, Materials Letters, china, 1665-1669, 2005.
15. C.Y.Huang, W.W.Mo, M.L. Roan, the influence of heat treatment on electroless-nickel coated fiber on the mechanical properties and EMI shielding of ENCF reinforced ABS polymeric composites, Surface Coatings Technology, Taiwan, 123-132, 2004.
16. D.T. Gawne, U.Ma, structure and waer of electroless nickel coatings, Institute of Metals, 228-238, 1986.
17. C.K. Chen, H.M. Feng, H.C Lin, M.H.Hon, the effect of heat treatment on the microstructure of electroless Ni-P coatings containing SiC particles, Thin Solid Films, 31-37, 2002.
18. I. Apachitei, E.D. Tichelaar, J. Duszcuzyk, L. Katgerman, the effect of heat treatment on the structure and abrasive wear resistance of autocatalytic NiP and NiP-SiC coatings, Surface and Coatings Technology, 263-278, 2001.
19. H. Ashassi-Sorkhabi, S.H. Rafizadeh, effect of coating time and heat treatment on structures and corrosion characteristics of electroless Ni-P alloy deposits, Surface and Coatings Technology, 318-326, 2004.
20. Z. Guo, K.G. Keong, W.Sha, crystallization and phase transformation behavior of electroless nickel phosphorus platings during continuous heating, Journal of Alloys and Compounds, 112-119, 2003.
21. Ray Taheri, Dr. Todd Pugsley, Evaluation of electroless nickel-phosphorous(EN) coatings, a thesis submitted to the college of graduate studies and research for the degree of doctor of philosophy, Department of Mechanical Engineering, university of Saskatchewan, canada, 2003.
22. S. Feih, K. Manatpon, Z. Mathys, A.G. Gibson, A.P. Mouritz, strength degradation of glass fibers at high tempratures, Material Science, 392-400, 2008.
23. D.J. Siconolfi, R.P. Frankenthal, air oxidation of a Ni-P, Journal of the Electrochemical Society, 1989.